Int. J. Appl. Ceram. Technol., 2 [1] 51–58 (2005)

International Journal of Applied Ceramic Technology
Ceramic Product Development and Commercialization

Characterization of the Piezoelectric Properties of $Pb_{0.98}Ba_{0.02}(Mg_{1/3}Nb_{2/3})O_3$–$PbTiO_3$ Epitaxial Thin Films

Jon-Paul Maria,[*,†] Joseph F. Shepard Jr.,[‡] and Susan Trolier-McKinstry[*,§]

The Pennsylvania State University Materials Research Institute, University Park, PA 16802

T. R. Watkins[*] and A. E. Payzant

Oak Ridge National Laboratory High Temperature Materials Laboratory, Oak Ridge, TN 37831

$Pb(Mg_{1/3}Nb_{2/3})O_3$–$PbTiO_3$ (PMN–PT) (70/30) thin films were deposited by pulsed laser deposition using two growth strategies: adsorption controlled deposition from lead-rich targets (~25–30 mass%) and lower-temperature deposition ($T_d \leq 600°C$) from targets containing a small amount of excess lead oxide (≤3 mass %). The substrates used were (001) $SrRuO_3/LaAlO_3$. Typical remanent polarization values ranged between 12 and 14 μC/cm^2 for these films. The longitudinal piezoelectric coefficient ($d_{33,f}$) was measured using *in situ* four-circle X-ray diffraction, and the transverse coefficient ($d_{31,f}$ or $e_{31,f}$) was measured using the wafer flexure method. $d_{33,f}$ and $e_{31,f}$ coefficients of ~300–350 pm/V and ~−11 C/m^2 were calculated, respectively. In general, the piezoelectric coefficients and aging rates were strongly asymmetric, suggesting the presence of a polarization bias. The large, extremely stable piezoelectric response that results from poling parallel to the preferred polarization direction is attractive for miniaturized sensors and actuators.

Introduction

There has been a growing interest in high piezoelectric coefficient thin films for microelectromechanical systems (MEMS).[1–3] A number of piezoelectric MEMS devices have been described in the literature, including accelerometers,[4] transducers and microactuators,[5–7] switches,[8] and motors.[9,10] To this point, most research efforts have focused on lead zirconate titanate (PZT) as the candidate ferroelectric film. Good piezoelectric coefficients have been obtained, with $e_{31,f}$ of −6 to −7 C/m^2 being typical of randomly oriented PZT 52/48 films. In contrast, some {100}-oriented films of the same composition show considerably larger $e_{31,f}$ values of about −12 C/m^2.[11]

Recently, ultra-large piezoelectric responses have been observed in rhombohedral single crystals of relaxor-$PbTiO_3$ solid solutions, including piezoelectric constants (d_{33}) of 2500 pC/N.[12,13] Thin films of $PbYb_{1/2}Nb_{1/2}O_3$–$PbTiO_3$ and $PbMg_{1/3}Nb_{2/3}O_3$–$PbTiO_3$

Work supported through NSF grants DMR-9502431 and DMR-0313764. Also supported by the Oak Ridge National Laboratory High Temperature Materials Laboratory.
*Member, American Ceramic Society.
†Present address: North Carolina State University, Raleigh, NC.
‡Present address: IBM Microelectronics Div., Hopewell Junction, NY.
§STMcKinstry@psu.edu

also show large $e_{31,f}$ values when grown with the (100) crystallographic orientation.[2,14] At present, however, there are no reports in the literature where the in- and out-of-plane piezoelectric response of relaxor-$PbTiO_3$ epitaxial films are reported. Such data are critical in determining the MEMS applications for such films should be suited. Higher piezoelectric coefficients offer the possibility of higher sensitivity sensors, as well as low voltage actuators. The latter, in particular, are quite important for being able to perform the driving with on-chip circuitry, which could motivate the integration of actuators into a number of "system-on-a-chip" applications.

Thus, it is the intent of this work to investigate the electromechanical behavior of the $Pb(Mg_{1/3}Nb_{2/3})O_3$–$PbTiO_3$ (PMN–PT) (70/30) solid solution when processed in the epitaxial thin film geometry. In doing so, it was necessary to develop methods for measuring the piezoelectric coefficients of small samples accurately. This article also details how this can be accomplished.

Sample Description

$Pb_{0.98}Ba_{0.02}(Mg_{1/3}Nb_{2/3})O_3$–$PbTiO_3$ (70/30) thin films were deposited by pulsed laser deposition on (001)-$LaAlO_3$ substrates; $SrRuO_3$ and Pt were used as the bottom and top electrodes, respectively. Two deposition strategies were used: adsorption-controlled growth with Pb supplied in excess, i.e., from targets containing ≤ 30 mass excess % PbO, and lower-temperature growth ($T_d < 600°C$) from targets containing ≤ 3 mass% excess PbO. These growth strategies were necessary to prepare epitaxial films with and without the influence of bombardment from energetic plasma species. The samples deposited using the adsorption-controlled process contained small amounts of both Pb-rich and Pb-deficient extra phases (at concentrations close to the detection limits of X-ray diffraction (XRD)), while the samples deposited using the lower-temperature parameters were phase pure to XRD. All samples exhibited high electrical resistivities (in excess of $10^8\ \Omega \cdot cm$) and low dielectric losses, sample thicknesses, as measured by profilometry, ranged between 0.5 and 1 μm. Table I summarizes the electrical properties typical of these samples. Full descriptions of the processing are given in the references.[15,16]

The longitudinal ($d_{33,f}$) and transverse ($e_{31,f}$) piezoelectric coefficients were measured using *in situ* field-dependent X-ray analysis and the wafer flexure method respectively, details of the measurement procedures are given in the discussion where pertinent.

Table I. Electrical Property Summary for PMN–PT Epitaxial Thin Films Deposited using Substrate Temperatures of ~670°C and ≤600°C

Property	$T_d \geq 670°C$	$T_d \leq 600°C$
P_r (μC/cm^2)	+17, −15	−1, −14
Permittivity	1500	1400
Loss tangent	3%	4%

The two values given for the remanent polarization correspond to the points where the hysteresis loop crosses the field axis.
†Permittivity and loss tangent measured at 1 kHz and 0.05 kV/cm.
PMN–PT, $Pb(Mg_{1/3}Nb_{2/3})O_3$–$PbTiO_3$.

Results and Discussion

Part I: In situ X-ray Analysis

Out-of-plane (or longitudinal) piezoelectric coefficients ($d_{33,f}$) were measured in this work by XRD. Here, the X-ray beam was confined to an electroded area and the diffraction angle corresponding to the interplanar spacing was measured as a function of the applied electric field. This method is attractive as it is not affected by wafer bending during piezoelectric drive (this type of wafer bending has been shown to complicate some interferometric measurements).[17] In addition, XRD has the potential to give field-dependent crystallographic information through peak shape analysis.

Due to the small sizes of the pulsed laser deposited PMN–PT heterostructure top electrodes (typically 0.3 or 0.5 mm in diameter), a 4-circle rotating anode instrument (Scintag PTS Rotating Anode) at the Oak Ridge National Laboratory, High Temperature Materials Laboratory Users Facility was used. The rotating anode generator was operated at powers in excess of 16 kW, with a 100 μm diameter collimator that could be aimed at the desired sample location.

Samples processed at temperatures above 670°C were used for the X-ray investigation. The diameter of the top electrodes was 500 μm. The samples were bonded to 16-pin chip-carriers, with connections between the film and chip-carrier electrodes made by aluminum wire bonding. A zip-dip socket was epoxied to the X-ray goniometer for electrical connection to an exterior power supply. The goniometer allowed *x*, *y*, and *z* translation

as well as rotation in the φ-circle. During X-ray scans, a field was applied to the samples from a 50 V dc power supply.

The samples were positioned in the desired location using the following procedure: first, a phosphor plate with a 300-μm pitch grid was positioned on the sample holder and adjusted to the appropriate height. With the 100 μm collimator in place, the beam was turned on, and its position on the grid was determined with a telescopic sight. With the beam off, a second telescopic sight was attached to the goniometer stage, and with respect to the reticule of the telescopic sight, the position of the grid point corresponding to the pre-determined beam location was found. The phosphor plate was removed, and a thin film sample was mounted. The height of the sample surface was brought into position using a micrometer gage. A second telescopic sight was remounted to the goniometer, and with the *x*–*y* translation controls, the desired electrode could be brought into the beam position as defined by the optics reticule. Figure 1 gives a schematic of the experimental setup, and a more complete discussion of the instrument can be found in the references.[18]

To measure the out-of-plane lattice strain with applied electric field, the 003 reflection was monitored as a function of dc bias on a sample that had previously been poled to 300 kV/cm. The 003 reflection was used as it provided appropriate intensity and was sufficiently separated in 2θ from substrate or electrode diffraction lines.

Angular steps of 0.02° and a scan time of 10 min were used. It was necessary to minimize the counting time and the subsequent duration of electric field application to minimize the occurrence of dielectric breakdown. Scans were performed at 0.5 V increments up to 5 V, and then larger increments to 30 V. Figure 2 shows the summary of these data (similar curves were produced using several samples).

From the strain-field plot in Fig. 2, a low dc bias field $d_{33,f}$ coefficient of approximately 300–350 pC/N can be calculated from the initial slope (< 20 kV/cm). Error bars were calculated from the uncertainty (± 0.001 Å) in *d*-spacing calculations. This value is established by the diffractometer resolution, the peak intensity, and the Diffraction Management Software (DMS) peak-fitting algorithm. Changes in peak shape were not detected at any field level. Note that the low bias $d_{33,f}$ value (~ 300–350 pm/V) is substantially higher than is typical of PZT thin films of similar thickness, which often show values between 50 and 150 pm/V.[2,17,19,20] This is not unreasonable, given the lower transition temperature of the PMN–PT films (~ 115°C rather than 350°C), thus the closer proximity to the ferroelectric transition at room temperature. At higher

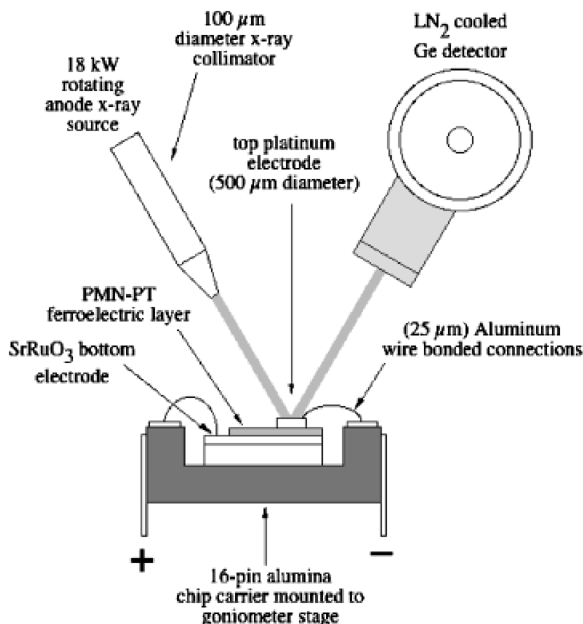

Fig. 1. Schematic illustration of in situ field-dependent X-ray analysis experimental setup.

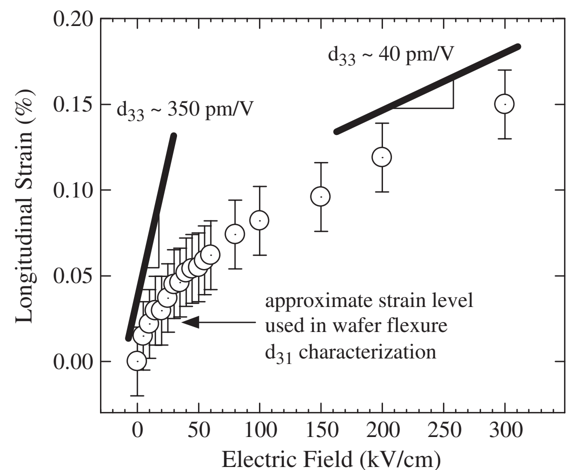

Fig. 2. Longitudinal piezoelectric strain for an epitaxial PMN–PT thin film deposited using the adsorption controlled method measured using in situ field-dependent X-ray diffraction.

fields, the $d_{33,f}$ coefficient reduces to a value of approximately 40 pm/V. There is no convincing evidence of a step in the strain or a change in the peak profile that would be indicative of a field-forced phase transition to the tetragonal phase of the type that has been reported in single crystals.

The piezoelectric coefficient is proportional to the product of the dielectric constant and the polarization. Ferroelectrics under dc bias show a substantial drop in the dielectric constant (i.e., tunability), which leads to a drop in the piezoelectric response. Thus, while the polarization may increase somewhat under dc field, the permittivity is dropping rapidly. X-ray measurements are completely static, so the tunability in the dielectric constant leads to a substantial reduction in the piezoelectric response measured at high dc fields. It is important to note that the field levels at which the piezoelectric coefficient levels off to 40 pm/V correspond to field values of about five times the coercive field, where the dielectric constant has dropped substantially. This accounts for at least some of the observed field dependence in the $d_{33,f}$ coefficient. Larger fields were not applied due to time-dependent dielectric breakdown of the samples. After reaching 300 kV/cm, the samples had been exposed to high fields for several hours. The maximum unipolar strain values recorded for PMN–PT samples (at $\sim$300 kV/cm) are similar to the reports of other researchers on PZT compositions under similar fields.[17]

Part II: Wafer Flexure Analysis

A modification of the wafer flexure method was used for $e_{31,f}$ (and $d_{31,f}$) characterization of PMN–PT samples.[21] The wafer flexure method relies on the ability to pressurize or evacuate a cavity to which a simply supported wafer is sealed. During this stress oscillation, a charge integrator is connected to the sample, which measures the piezoelectric charge, and allows calculation of the stress-induced polarization.

In order to apply this technique, a modification was necessary due to the relatively small sizes of the PMN–PT samples (typically $\leq 1\ cm^2$). The modification involved bonding the small single crystal substrates to Si wafers, and relying on strain transfer through the bonding layer to achieve a biaxial stress on the PMN–PT surface. The strain on the PMN–PT surface during pressure oscillation was measured for reference samples with foil resistance strain gages. The small samples

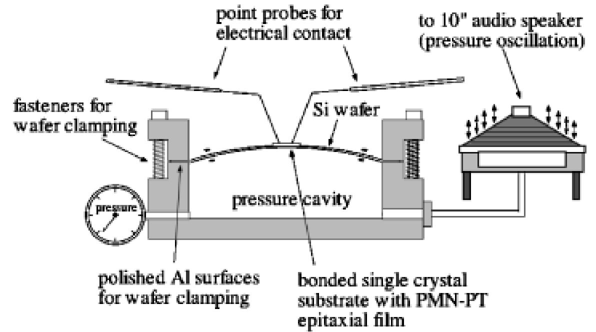

Fig. 3. Schematic of wafer-flexure experimental setup.

(hereafter referred to as chips) as well as the strain gages were bonded using a cyanoacrylate adhesive. A schematic representation of the wafer-flexure rig is illustrated in Fig. 3.

A strain calibration was performed for an $LaAlO_3$ substrate bonded to Si. Figure 4 shows a plot of the strain measured on the surface of the $LaAlO_3$ chip as a function of speaker oscillation voltage. The linear dependence of strain with cavity pressure is indicative of the integrity of the bonding layer, as nonlinearity would be expected were delamination or plastic deformation occurring. A linear relationship is also predicted from small-deflection plate theory.[13]

The output of the strain gage conditioner was sent to a lock-in amplifier that drove the pressure oscillation. Using this arrangement, an rms strain was determined. For all measurements the audio speaker was driven

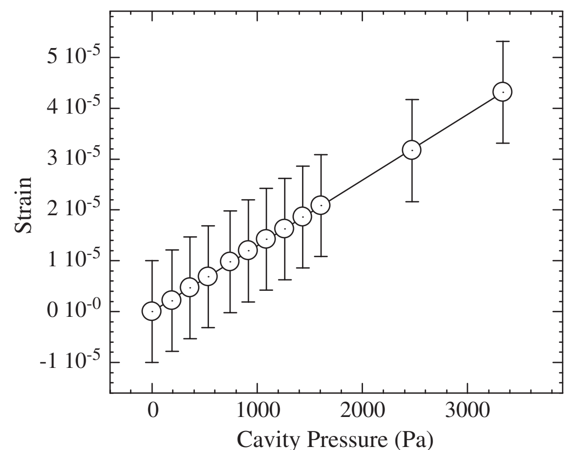

Fig. 4. Calibration plot for wafer-flexure apparatus showing the uniaxial strain as a function of static cavity pressure.

at 0.5 V, which corresponded to an rms strain of $1.5 \times 10^{-5} \pm 0.1 \times 10^{-5}$. A second calibration experiment was performed where an $LaAlO_3$ wafer of approximately 50% smaller area was used. A similar strain calibration was undertaken and it was determined that the reduced wafer size did not result in an appreciable change in strain for the same pressure oscillation. All chips used for piezoelectric measurement had dimensions that were between those of the chips used for strain calibration.

To check the quality of the resulting data, a polycrystalline PZT/Pt/Ti/SiO_2/Si thin film chip with known piezoelectric coefficients was bonded to the center of a 75-mm Si wafer. A strain gage was bonded to the chip surface, and the uniaxial strain was measured for several pressure oscillation levels. In all of the bonding operations, care was taken to orient all Si and $LaAlO_3$ wafers and chips such that the crystallographic directions were aligned (i.e., [100] $LaAlO_3$//[100] Si or [100] Si//[100] Si). The strain gages were aligned such that the strain measurement direction was directed along the [100] crystallographic axis. In addition, the crystals were all roughly square in shape and positioned in the center of the Si wafer. As a check, a second calibration of the piezoelectric coefficients was carried out using a PZT-coated chip and a full PZT-coated wafer. The results on the two samples agreed within the accuracy of the technique. The details of the calculation and measurement procedure were identical to those developed by Shepard *et al.*[21]

A limitation in the accuracy of the derived $d_{31,f}$ piezoelectric coefficients is that knowledge of the elastic constants is required for the calculation. Elastic constants were not measured for the PMN–PT thin films; however, reference data for single crystals of the same composition were available. The pertinent Young's modulus, E_{11} has been measured by ultrasonic techniques for PMN–PT (70/30) single crystals; a value of 40 GPa was determined and used in calculations of $d_{31,f}$.[22] The possibility exists that the elastic constants of the thin film samples are appreciably different than those of single crystals, especially when considering doping, residual stress, second phase, and composition effects. However, in oriented PMN–PT (70/30) sol–gel films on Si, an in-plane Young's modulus of 44 GPa was estimated, in reasonable agreement with the value used here.[23] To avoid this difficulty with uncertainty in the film elastic properties, $e_{31,f}$ values are preferable, and are noted throughout the article.[3]

Wafer flexure measurements were made for samples grown at high temperatures (~670°C), and those deposited below 600°C. For each sample type, two sets of data are presented: poling plots, where the piezoelectric coefficient is given as a function of poling time, and aging plots, where the piezoelectric coefficient is given as a function of time after removal of the poling field. During the aging experiments, the pressure oscillation was continuous, with the top electrode contact removed. This was required to avoid errors stemming from the instability of the pressure oscillation during the initial cycles. In contrast, during the poling experiments, the oscillation was turned off. This was necessary to avoid excessive wear to the top electrode surface via scratching with the metal point probe tip. To eliminate the instability of the oscillation pressure during the initial cycles, a voltage output was recorded one minute after the oscillation began. Poling voltages of 5 V (50 kV/cm) were used in all cases. The corresponding fields are approximately twice the coercive field value; larger voltages were not applied as poling occurred too rapidly for the observation of any systematic trends with time.

Figure 5 shows the poling curve for a PMN(2% Ba)–PT (70/30) thin film deposited at 670°C, where data are given for poling in both directions, i.e., top electrode positive and negative. In all cases, the $e_{31,f}$ (and $d_{31,f}$) coefficients are all given as negative; thus, the poling directions are differentiated by the measurement phase angle. The angle (θ) corresponds to phase difference between the periodic signals produced by the pressure oscillation drive and the integrated piezoelectric

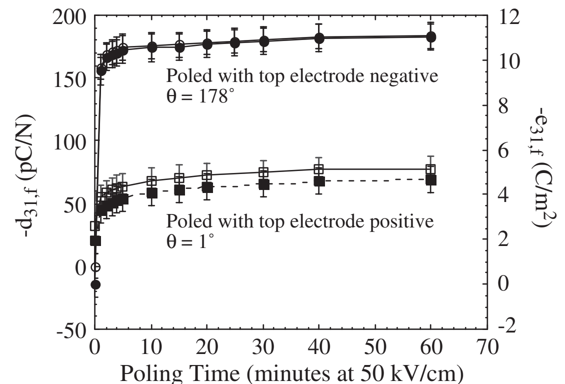

Fig. 5. $-d_{31,f}$ (open symbols) and $e_{31,f}$ (filled symbols) as a function of poling time for a PMN–PT epitaxial film deposited using the adsorption-controlled method. Data are given for both top-electrode-positive and top-electrode-negative poling directions.

charge. As such, the phase angle should switch by 180° when the poling direction is reversed. The error bars indicate the ability to resolve an rms voltage on the lock-in amplifier, the measurement accuracy of the top electrode area, and the uncertainty in the strain analysis. Potential errors in $d_{31,f}$ associated with knowledge of the elastic constants are not included.

The asymmetry of the piezoelectric properties in Fig. 5 is pronounced in the poling curves and suggestive of an internal polarization bias. In the case of these samples, the direction of the preferred polarization is from the film/substrate interface to the surface, as evidenced by the larger piezoelectric coefficients achievable after poling with the top electrode negative. Figure 6 shows the aging data for the same sample; again, evidence for a strong internal bias is observed. For poling in the direction of the internal bias, the aging rate is effectively zero; even when films were remeasured following aging for more than one week, negligible reductions in $e_{31,f}$ ($d_{31,f}$) were observed. When the aging rate was measured for poling against the internal bias, rates as large as 30%/decade were determined. Such large values are likely associated with the internal polarization bias.

The same set of experiments were performed on the samples deposited at temperatures below 600°C. Figure 7 contains the poling information, again for top electrode positive and top electrode negative poling conditions. The same type of asymmetry is observed for this

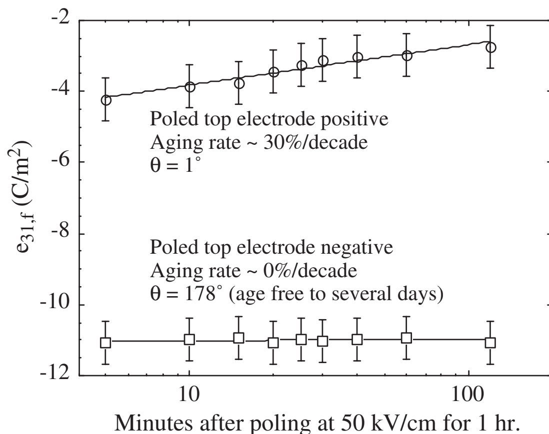

Fig. 6. $-e_{31,f}$ *as a function of aging time for PMN–PT epitaxial film deposited using the adsorption controlled method. Data are given for both top-electrode-positive and top-electrode-negative poling directions.*

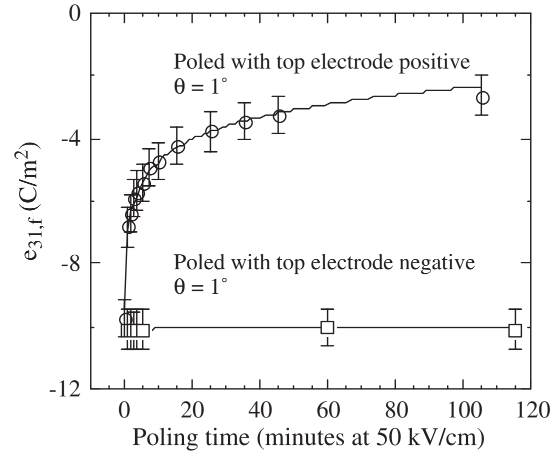

Fig. 7. $-e_{31,f}$ *as a function of poling time for PMN–PT epitaxial film deposited at temperatures below 600°C. Data are given for both top-electrode-positive and top-electrode-negative poling directions.*

film; however, the differences between the poling conditions are even more stark. The phase angle observed for both poling directions is $\sim 1°$, which indicates that the direction of the remanent polarization cannot be switched by room temperature poling. Larger field values were applied for longer time periods in an attempt to achieve a zero state of poling, however, all attempts resulted in electrical breakdown (breakdown typically occurred after application of dc fields in excess of 500 kV/cm). This is in contrast to the high-temperature deposited samples that could be taken through $d_{31,f} \sim 0$ pC/N with the appropriate electric field application.

To make sure that the inability to switch the phase angle of the measurement was not an artifact of the technique, a dc bias was applied to the film in the direction opposite to the internal bias and the piezoelectric coefficient was measured. As expected, at a field of approximately 100 kV/cm, the phase angle switched to a value of 179°.

As before, the sample was allowed to age and the results of this test are given in Fig. 8. After poling in the direction of the internal bias, a negligible aging rate was observed for times in excess of one week. When the aging measurement was performed for the poling condition opposite to the internal bias, a positive aging rate was recorded. That is, the piezoelectric coefficient increased in magnitude over time with respect to the as-poled situation. Asymmetric piezoelectric properties have been observed in numerous previous reports;

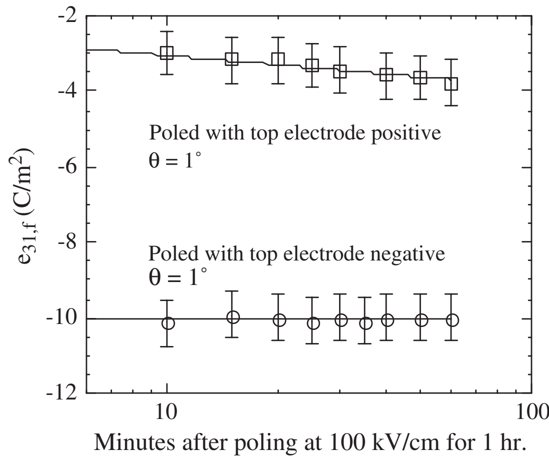

Fig. 8. $-e_{31,f}$ as a function of aging time for PMN–PT epitaxial film deposited at temperatures below 600°C. Data are given for both top-electrode-positive and top-electrode-negative poling directions.

however, this is believed to be the first observation of a positive aging rate in a ferroelectric thin film.

When poled in the direction of the preferred polarization orientation, PMN–PT films deposited using both approaches exhibited $e_{31,f}$ between -10 and $-11\,C/m^2$ ($d_{31,f}$ piezoelectric coefficients of about -160 and -180 pC/N). These numbers are similar to those seen in {100} PZT films at the morphotropic phase boundary,[3,11] and substantially larger than is typical of randomly oriented PZT films.[21,24] Similar results were demonstrated for multiple samples, and multiple top electrodes on each sample.

The asymmetric electrical behavior is also observed in the hysteresis data (given in Table I). For the material deposited at temperatures in excess of 670°C, a modest shift exists on the field axis of the hysteresis loop; however, the remanent polarization states are of opposite sign. This is consistent with the piezoelectric data, which indicates that a larger piezoelectric coefficient can be achieved in one direction, and that the net orientation of the remanent polarization can be reversed. For the material deposited at lower temperatures and pressures, the shift along the field axis is large enough such that both remanent polarization states have the same sign. This agrees with the piezoelectric data, where in the absence of large dc bias fields, the phase angle for the measurement could not be switched from 0° to 180° despite changing the poling polarity. The origins of these polarization bias effects as well as the details of the processing are discussed elsewhere.[15]

The reduction in aging rates for the films with a strong preference for a particular polarization state is consistent with observations in sol–gel films that have been deliberately imprinted.[25] The extremely large asymmetry observed in the pulsed laser deposited films suggests that energetic particle bombardment during growth may be particularly effective in stabilizing the film response both against aging and against large ac drive levels.

A comparison can be made between the piezoelectric data calculated using both techniques, following the approximate relationship between d_{33} and $-d_{31}$ (i.e., d_{33} to $-2\ d_{31}$).[26] In Fig. 2, the approximate strain level corresponding to that used during the wafer flexure analysis is indicated by an arrow. As mentioned, the $-d_{31,f}$ coefficient estimated for this strain level was between 160 and 180 pC/N. This value is approximately 50% smaller than the calculated low-field d_{33} coefficient, and indicates a reasonable self-consistency between measurements. It also suggests that there was little cracking or porosity in the films, as an increase in the ratio of $d_{33,f}/e_{31,f}$ is characteristic of films with poor mechanical continuity in the plane.

Summary and Conclusions

Both the longitudinal and transverse piezoelectric coefficients were measured for PMN(2% Ba) –PT (70/30) epitaxial thin films. Low field values for the $d_{33,f}$ and $e_{31,f}$ coefficients were determined to be $\sim$300–350 pm/V and $\sim -11\,C/m^2$ respectively. The low-field piezoelectric response is approximately 2 to 4 times stronger than reports for randomly oriented PZT films of similar thickness. The results of the techniques are in reasonable agreement, as a general relationship between the magnitude of d_{33} and $-d_{31}$ of $\sim$2:1 is observed.

Longitudinal strains as large as 0.15% were observed at a dc field of 300 kV/cm. Larger fields could not be used due to breakdown of the samples. These strains were similar in magnitude to those measured for polycrystalline PZT thin films, but much smaller than those measured for bulk relaxor-PT single crystals. The small $d_{33,f}$ coefficient values (in comparison with single-crystal reports) may be associated with substrate clamping and residual stress. In addition, the inferior crystallinity of thin films, as compared with bulk single

crystals, and the possibility of nano-scopic phase impurity likely contribute to the comparatively weak response. This being the case, films deposited on better lattice-matched substrates, or those deposited with further process optimizations may exhibit better electromechanical properties.

From $e_{31,f}$ measurements, the polarization state of the PMN–PT thin films was found to be orientationally biased. For films deposited at temperatures in excess of 670°C, a preferred polarization orientation was found. For films deposited below 600°C, the polarization bias was large enough such that with room temperature poling, the direction of the remanent polarization could not be switched (i.e., both remanent polarization values carried the same sign). For these samples, poling in the direction of the internal bias resulted in very rapid saturation of $e_{31,f}$, and piezoelectric coefficients that had extremely low aging rates. Rapid aging was observed for samples poled against the as-grown bias.

References

1. D. L. Polla and L. F. Francis, "Processing and Characterization of Piezoelectric Materials and Integration into Microelectromechanical Systems," *Annu. Rev. Mater. Sci.*, 28 563–597 (1998).
2. S. Trolier-McKinstry and P. Muralt. "Thin Film Piezoelectrics for MEMS," *J. Electroceram.*, 12 7–17 (2004).
3. P. Muralt, "PZT Thin Films for Microsensors and Actuators: Where do We Stand?," *IEEE T. UFFC*, 47 [4] 903–915 (2000).
4. L.-P. Wang, R. A. Wolf, W. Yu, K. K. Deng, L. Zou, R. J. Davis, and S. Trolier-McKinstry, "Design, Fabrication, and Measurement of High-sensitivity Piezoelectric Microelectromechanical Systems Accelerometers," *J. MEMS*, 12 [4] 433–439 (2003).
5. J. J. Bernstein, S. L. Finberg, K. Houston, L. C. Niles, H. D. Chen, L. E. Cross, K. K. Li, and K. Udayakumar, "Micromachined High Frequency Ferroelectric Sonar Transducers," *IEEE Trans. UFFC*, 44 [5] 960–969 (1997).
6. Y. Miyahara, M. Deschler, T. Fujii, S. Watanabe, and H. Bleuler, "Non-contact Atomic Force Microscope with a PZT Cantilever used for Deflection Sensing, Direct Oscillation and Feedback Actuation," *Appl. Surf. Sci.*, 188 [3–4] 450–455 (2002).
7. Y. Yee, H. J. Nam, S. H. Lee, J. U. Bu, and J. W. Lee, "PZT Actuated Micromirror for Fine-tracking Mechanism of High-density Optical Data Storage," *Sensor. Actuat. A*, 89 [1–2] 166–173 (2001).
8. S. J. Gross, S. Tadigadapa, T. N. Jackson, S. Trolier-McKinstry, and Q. Q. Zhang, "Lead-Zirconate-Titanate-Based Piezoelectric Micromachined Switch," *Appl. Phys. Lett.*, 83 [1] 174–176 (2003).
9. M. A. Dubois and P. Muralt, "PZT Thin Film Actuated Elastic Fin Micromotor," *IEEE T. UFFC*, 45 [5] 1169–1177 (1998).
10. T. Morita, M. K. Kurosawa, and T. Higuchi, "A Cylindrical Shaped Micro Ultrasonic Motor Utilizing PZT Thin Film (1.4 mm in diameter and 5.0 mm long stator transducer)," *Sensor. Actuat. A*, 83 [1–3] 225–230 (2000).
11. N. Ledermann, P. Muralt, J. Baborowski, S. Gentil, K. Mukati, M. Cantoni, A. Seifert, and N. Setter, "{100}-Textured, Piezoelectric $Pb(Zr_xTi_{1-x})O_3$ Thin Films for MEMS: Integration, Deposition, and Properties," *Sensor. Actuat. A*, 105 [2] 162–170 (2003).
12. S. E. Park and T. R. Shrout, "Ultrahigh Strain and Piezoelectric Behavior in Relaxor Based Ferroelectric Single Crystals," *J. Appl. Phys.*, 82 [4] 1804–1811 (1997).
13. S. Trolier-McKinstry, L. E. Cross, and Y. Yamashita, eds. *Piezoelectric Single Crystals and Their Application*. S. Trolier-McKinsky, University Park, PA, 2004.
14. T. Yoshimura and S. Trolier-McKinstry, "Growth and Piezoelectric Properties of $Pb(Yb_{1/2}Nb_{1/2})O_3$–$PbTiO_3$ Epitaxial Films," *J Appl. Phys.*, 92 [7] 3979–3984 (2002).
15. J-P. Maria, W. Hackenberger, and S. Trolier-McKinstry, "Phase Development and Electrical Property Analysis of Pulsed Laser Deposited $Pb(Mg_{1/3}Nb_{2/3})O_3$–$PbTiO_3$ (70/30) Epitaxial Films," *J. Appl. Phys.*, 84 [9] 5147–5154 (1998).
16. J-P. Maria, S. Trolier-McKinstry, D. G. Schlom, M. E. Hawley, and G. W. Brown, "The Influence of Energetic Bombardment on the Structure and Properties of Epitaxial $SrRuO_3$ Thin Films Grown by Pulsed Laser Deposition," *J. Appl. Phys.*, 83 [8] 4373–4379 (1998).
17. A. L. Kholkin, C. Wütchrich, D. V. Taylor, and N. Setter, "Interferometric Measurements of Electric field-induced Displacements in Piezoelectric Thin Films," *Rev. Sci. Instrum.*, 67 [5] 1935–1941 (1996).
18. M. Y. Inal, M. Alam, R. A. Peascoe, and T. R. Watkins, "Residual Stress in Deuterium Implanted Nominal Copper Coatings," *J. Appl. Phys.*, 88 [7] 3919–3925 (2000).
19. F. Xu, S. Trolier-McKinstry, W. Ren, and B. Xu, "Domain Wall Motion and its Contribution to the Dielectric and Piezoelectric Properties of Lead Zirconate Titanate Films," *J. Appl. Phys.*, 89 [2] 1336–1348 (2001).
20. D. V. Taylor and D. Damjanovic, "Piezoelectric Properties of Rhombohedral $Pb(Zr, Ti)O_3$ Thin Films with (100), (111), and "Random" Crystallographic Orientation," *Appl. Phys. Lett.*, 76 [12] 1615–1617 (2000).
21. J. F. Shepard Jr., P. J. Moses, and S. Trolier-McKinstry, "The Wafer Flexure Technique for the Determination of the Transverse Piezoelectric Coefficient (d_{31}) of PZT Thin Films," *Sensor. Actuat. A* 71 133–138 (1998).
22. S. E. Park and T. R. Shrout, Unpublished material, 1997.
23. J. H. Park, F. Xu, and S. Trolier-McKinstry, "Dielectric and Piezoelectric Properties of Sol–Gel Derived Lead Magnesium Niobium Titanate Films with Different Textures," *J. Appl. Phys.*, 89 [1] 568–574 (2001).
24. R. A. Wolf and S. Trolier-McKinstry, "Temperature Dependence of the Piezoelectric Response in Lead Zirconate Titanate Films," *J. Appl. Phys.*, 95 [3] 1397–1406 (2004).
25. R. G. Polcawich and S. Trolier-McKinstry, "Piezoelectric and Dielectric Reliability of Lead Zirconate Titanate Thin Films," *J. Mater. Res.*, 15 [11] 2505–2513 (2000).
26. B. Jaffe, W. R. Cook, and H. Jaffe, *Piezoelectric Ceramics*. R. A. N. Publishers, Marietta, OH, 1971.